

## An improved criterion for Kapitza's pendulum stability

This article has been downloaded from IOPscience. Please scroll down to see the full text article.

2011 J. Phys. A: Math. Theor. 44 295202

(<http://iopscience.iop.org/1751-8121/44/29/295202>)

View [the table of contents for this issue](#), or go to the [journal homepage](#) for more

Download details:

IP Address: 92.100.102.149

The article was downloaded on 20/06/2011 at 14:37

Please note that [terms and conditions apply](#).

# An improved criterion for Kapitza's pendulum stability

**Eugene I Butikov**

St. Petersburg State University, St. Petersburg, Russia

E-mail: [eugene.butikov@gmail.com](mailto:eugene.butikov@gmail.com)

Received 24 March 2011, in final form 5 May 2011

Published 17 June 2011

Online at [stacks.iop.org/JPhysA/44/295202](http://stacks.iop.org/JPhysA/44/295202)

## Abstract

An enhanced and more exact criterion for dynamic stabilization of the parametrically driven inverted pendulum is obtained: the boundaries of stability are determined with greater precision and are valid in a wider region of the system parameters than previous results. The lower boundary of stability is associated with the phenomenon of subharmonic resonances in this system. The relationship of the upper limit of dynamic stabilization of the inverted pendulum with ordinary parametric resonance (i.e. with destabilization of the lower equilibrium position) is established. Computer simulation of the physical system aids the analytical investigation and proves the theoretical results.

PACS numbers: 05.45.-a, 05.10.-a, 07.05.Tp, 45.10.-b

## 1. Introduction

A well-known curiosity of classical mechanics is the dynamic stabilization of an inverted pendulum. An ordinary rigid planar pendulum whose pivot is forced to oscillate along the vertical line becomes stable in the inverted position if the driving amplitude and frequency lie in certain intervals. At small and moderate deviations from the inverted position, the pendulum shows no tendency to turn down. Being deviated, the pendulum executes relatively slow oscillations about the vertical line on the background of rapid oscillations of the suspension point. Due to friction these slow oscillations gradually damp away, and the pendulum eventually comes to rest in the vertical inverted position.

This type of dynamic stability was probably first pointed out by Stephenson [1] more than a century ago. In 1951, such extraordinary behavior of the pendulum was physically explained and investigated experimentally in detail by Pjotr Kapitza [2], and the corresponding physical device is now widely known as 'Kapitza's pendulum'. Since then, this intriguing system has attracted the attention of many researchers, and the theory of the phenomenon may seem to be well elaborated—see, for example, [3]. A vast list of references on the subject can be found in [4]. Nevertheless, more and more new features in the behavior of this apparently inexhaustible system are reported regularly.

Among new discoveries regarding the inverted pendulum, the most important for finding the stability boundaries are the destabilization of the (dynamically stabilized) inverted position at large driving amplitudes through excitation of period-2 ('flutter') oscillations [5, 6], and the existence of  $n$ -periodic 'multiple-nodding' regular oscillations [7]. The relationship of 'flutter' oscillations in the inverted pendulum with ordinary parametric resonance of the hanging pendulum is discussed in [8]. A physical interpretation of periodic multiple-nodding oscillations as subharmonic parametric resonances is given in [9].

In this paper, we present an improved criterion for dynamic stabilization of the parametrically driven inverted pendulum. The lower boundary of the parameter space region in which the inverted pendulum can be stable is associated with conditions of subharmonic resonance of an infinitely large order. The upper boundary is related to a certain branch of excitation of ordinary parametric resonance. These relationships allow us to determine the boundaries of dynamic stabilization in a wider region of the system parameters (including relatively low frequencies and large amplitudes of excitation), and with a greater precision compared to previous results.

## 2. The physical system

We consider for simplicity a light rigid rod of length  $l$  with a heavy small bob of mass  $M$  on its end and assume that all the mass of the pendulum is concentrated in the bob. The force of gravity  $Mg$  (here  $g$  is the free fall acceleration) provides a restoring torque  $-Mgl \sin \varphi$  whose value is proportional to the sine of angular deflection  $\varphi$  of the pendulum from the lower equilibrium position. With the suspension point at rest, this torque makes the deviated pendulum to swing about the lower stable equilibrium position. When the axis of the pendulum is constrained to move with acceleration along the vertical line, it is convenient to analyze the motion in the non-inertial reference frame associated with this axis. Due to the acceleration of this frame of reference, the pseudoforce of inertia  $-M\ddot{z}$  is exerted on the pendulum, where  $z(t)$  is the vertical coordinate of the axis. The torque of this force  $-M\ddot{z}l \sin \varphi$  must be added to the torque of the gravitational force.

We assume that the axis is forced to execute a given harmonic oscillation along the vertical line with frequency  $\omega$  and amplitude  $a$ :  $z(t) = a \cos \omega t$ . The force of inertia  $F_{\text{in}}(t)$  exerted on the bob in the non-inertial frame of reference also has the same sinusoidal dependence on time:

$$F_{\text{in}}(t) = -M\ddot{z}(t) = M\omega^2 z(t). \quad (1)$$

This force of inertia is directed upward during the time intervals for which  $z(t) > 0$ , i.e. when the axis is over the middle point of its oscillations. Therefore, during the corresponding half-period of the oscillation of the pivot, this additional force is equivalent to some weakening of the force of gravity. During the other half-period, the axis is below its middle position ( $z(t) < 0$ ), and the action of this additional force is equivalent to some strengthening of the gravitational force.

The graphs of time history and the phase trajectories for different modes of the pendulum that are presented further in this paper are obtained by a numerical integration of the exact differential equation for angular deflection  $\varphi(t)$  of the pendulum with the oscillating pivot. This equation includes, besides the torque  $-Mg \sin \varphi$  of the gravitational force  $Mg$ , the torque of the force of inertia  $F_{\text{in}}(t)$  which depends explicitly on time  $t$ :

$$\ddot{\varphi} + 2\gamma\dot{\varphi} + \left( \frac{g}{l} - \frac{a}{l}\omega^2 \cos \omega t \right) \sin \varphi = 0. \quad (2)$$

The second term in (2) originates from the frictional torque which is assumed in this model to be proportional to the momentary value of the angular velocity  $\dot{\varphi}$ . The damping constant  $\gamma$  in this term is inversely proportional to the quality factor  $Q$  which is conventionally used to characterize damping of small natural oscillations under viscous friction:  $Q = \omega_0/2\gamma$ , where  $\omega_0 = \sqrt{g/l}$  is the frequency of infinitely small natural oscillations in the absence of pivot oscillations.

Oscillations about the inverted position can be formally described by the same differential equation (2) with negative values of  $g$ , as if the force of gravity were directed upward. In other words, we can treat the free fall acceleration  $g$  in equation (2) as a control parameter whose variation is physically equivalent to the variation of the gravitational force. When this control parameter  $g$  is diminished through zero to negative values, the gravitational torque in (2) also reduces down to zero and then changes its sign to the opposite. Such a ‘gravity’ tends to bring the pendulum into the inverted position  $\varphi = \pi$ , destabilizing the lower equilibrium position  $\varphi = 0$  of the unforced pendulum and making the upper position  $\varphi = \pi$  stable: at  $g < 0$  the inverted position in (2) is equivalent to the lower position at positive  $g$ .

### 3. An approximate criterion of stability

Since the first works of Kapitza [2], stabilization of the inverted pendulum is usually explained by the method of averaging based on a heuristic approach, according to which the pendulum motion is represented as a relatively slow oscillation described by a smooth function  $\psi(t)$ . The slow motion is distorted by superposition of rather small fast vibrations  $\delta(t) \ll 1$  of a high frequency:

$$\varphi(t) = \psi(t) + \delta(t) \approx \psi(t) - \frac{z(t)}{l} \sin \psi = \psi(t) - \frac{a}{l} \sin \psi \cos \omega t. \quad (3)$$

The rapidly varying component  $\delta(t)$  in the above expression for  $\varphi(t)$  is obtained on the assumption that during one period  $T$  of fast vibration of the pivot, the slow component  $\psi$  remains almost constant. In this approximation, the time dependence of  $\delta(t)$  in (3) can be easily seen from figure 1: when the oscillating pivot  $A$  is displaced from its mid-point through some distance  $z$  for a given angle  $\psi$ , the momentary angle  $\varphi$  acquires an additional value of approximately  $-(z/l) \sin \psi$ .

Figure 1 shows the pendulum at the utmost displacements of the pivot in the inertial (upper part *a*) and non-inertial (lower part *b*) frames. In the non-inertial frame associated with the pivot, the bob of the pendulum moves up and down along an arc of a circle and occurs in positions 1 and 2 at the instants at which the oscillating axis reaches its extreme positions 1 and 2, respectively, shown in the upper part of figure 1. We note that the rod has the same simultaneous orientations in both reference frames at instant 1 as well as at instant 2. When the pivot is displaced downward to position 2 from its midpoint, the force of inertia  $F_2$  exerted on the bob is also directed downward. In the other extreme position 1, the force of inertia  $F_1$  has an equal magnitude and is directed upward. However, the *torque* of the force of inertia in position 1 is greater than in position 2 because the *arm* of the force in this position is greater. Therefore, on average, the force of inertia creates a torque about the axis that tends to turn the pendulum upward, into the vertical inverted position, in which the rod is parallel to the direction of oscillations.

This simple qualitative physical explanation of the phenomenon of dynamic stabilization can be supported by approximate quantitative considerations. The momentary torque of the force of inertia  $F_{in}(t)$  is given by the product of this force (1) and its arm  $l \sin \varphi(t) \approx l \sin \psi + l \cos \psi \delta(t)$ . Averaging this torque over the period  $T$  of rapid oscillations of the

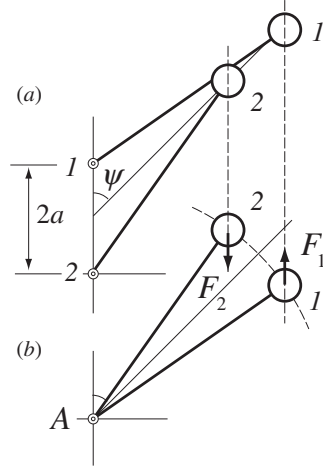


**Figure 1.** Behavior of the pendulum with an oscillating axis in the inertial reference frame (a) and in the frame associated with the pivot (b).

pivot, we can regard the slow angular coordinate  $\psi(t)$  to be constant:  $\psi(t) \approx \psi$ . In this approximation, the first term of the mean torque  $\langle F_{in}(t) l \sin \psi \rangle$  vanishes due to the zero average value  $\langle F_{in}(t) \rangle$  of the force of inertia, while the second term gives

$$\langle F_{in}(t) l \cos \psi \delta(t) \rangle = -Ma^2\omega^2 \sin \psi \cos \psi \langle \cos^2 \omega t \rangle = -\frac{1}{2}Ma^2\omega^2 \sin \psi \cos \psi. \quad (4)$$

This mean torque of the force of inertia at  $\psi > \pi/2$  tends to bring the pendulum into the inverted position. It can exceed in magnitude the torque  $-Mgl \sin \psi$  of the gravitational force that tends to tip the pendulum down when the following condition is fulfilled:

$$a^2\omega^2 > 2gl, \quad \text{or} \quad \frac{a}{l} \cdot \frac{\omega}{\omega_0} > \sqrt{2}, \quad \text{or} \quad \frac{a}{l} > \sqrt{-2k}, \quad (5)$$

where  $\omega_0 = \sqrt{g/l}$  is the frequency of infinitely small natural oscillations of the pendulum. This is the commonly known (approximate) criterion of the inverted pendulum stability. In the perspective of the forthcoming generalization and improvement, we have also expressed in (5) this criterion in terms of parameter  $k$ , which is defined by the following expression:

$$k = \frac{\omega_0^2}{\omega^2} = \frac{g}{l\omega^2}. \quad (6)$$

This dimensionless parameter  $k$  (inverse normalized drive frequency squared), being physically less meaningful than  $\omega/\omega_0$ , is nevertheless more convenient for further investigation, because the improved criterion acquires a simpler form in terms of  $k$ . Negative values of  $k$  correspond to negative  $g$  values, which can be formally assigned to the inverted pendulum, as we have already noted earlier.

The above-discussed approach based on the separation of slow and rapid components of the pendulum motion is applicable for relatively small amplitudes and high frequencies of the pivot oscillations. Hence, the commonly known expressions (5) for stability criteria are valid only at  $\omega/\omega_0 \gg 1$  and  $a/l \ll 1$ .

#### 4. Subharmonic resonances of high orders and stability of the inverted pendulum

An alternative way to obtain the stability criterion for the inverted pendulum is based on the relationship between damping oscillations about the inverted position and stationary regimes of subharmonic oscillations [9]. This approach allows us to find a more exact and enhanced criterion which is valid in a wider, compared with conventional criterion (5), region of the system parameters. In particular, this improved criterion can be used for relatively large amplitudes and low frequencies of the pivot oscillations for which the method of averaging is inapplicable.

When the amplitude and frequency of the pivot oscillations lie within certain ranges, the pendulum, instead of gradually approaching the equilibrium position (either dynamically stabilized inverted position or ordinary downward position) by the process of damped slow oscillations, can be trapped into an  $n$ -periodic limit cycle. By virtue of the ‘phase locking’ (synchronization of oscillations of the pendulum with those of the pivot, characterized by certain relationship between their phases), the pendulum is regularly fed by additional energy to compensate for frictional losses. The phase trajectory exactly repeats itself after  $n$  periods  $T$  of excitation are finished. One period of such non-damping oscillations of the dissipative pendulum equals exactly an integer number of cycles ( $n$ ) of the pivot vibrations. The frequency  $\omega/n$  of the principal harmonic equals  $1/n$  of the excitation frequency  $\omega$ . This allows us to call this phenomenon a subharmonic resonance of order  $n$ .

For the inverted pendulum with a vibrating pivot, periodic oscillations of this type were first described by Acheson [7], who called them ‘multiple-nodding’ oscillations. Computer simulations show that the pendulum motion in this regime reminds us of some kind of an original dance. Similar ‘dancing’ oscillations can be executed also (at appropriate values of the driving parameters) about the ordinary equilibrium position [8]. ‘Multiple-nodding’ oscillations can occur also in the absence of gravity about any of the two equivalent dynamically stabilized equilibrium positions [9].

An example of such a subharmonic resonance (regular period-8 steady-state motion of the pendulum) is shown in figure 2. One period of the pendulum motion covers exactly eight cycles of the pivot oscillations. Poincaré sections on the phase orbit mark the mechanical state ( $\varphi, \dot{\varphi}$ ) of the pendulum once during each cycle of the excitation. The set of these sections (Poincaré map) consists of eight fixed points in the phase plane visited by the representing point in a definite sequence. The sections on the spatial and phase orbits in figure 2 are marked by integer numbers  $q = 0, 1, 2 \dots$  that correspond to the time instants on the time scale at which  $q$  drive periods  $T = 2\pi/\omega$  are completed.

A simple approximate derivation of conditions at which multiple-nodding oscillations are possible can be based on the effective potential concept [8, 9]. The natural slow oscillatory motion in the effective potential well is almost periodic (exactly periodic in the absence of friction). The pendulum can be trapped in a limit cycle of order  $n$  if one cycle of this slow motion covers approximately  $n$  driving periods, that is, when the driving frequency  $\omega$  is close to an integer multiple  $n$  of the natural frequency  $\omega_{\text{up}}$  or  $\omega_{\text{down}}$  of slow oscillations near either the inverted or the ordinary equilibrium position, respectively. For small amplitudes of the slow oscillations, each of the minima of the effective potential (at  $\varphi = 0$  and at  $\varphi = \pi$ ) can be approximated by a parabolic well in which the smooth component of motion is almost harmonic. Equating its frequency  $\omega_{\text{up}}$  or  $\omega_{\text{down}}$  [9] to  $\omega/n$ , we find the threshold (low-amplitude) conditions for the subharmonic resonance of order  $n$ :

$$m_{\min} = \sqrt{2(1/n^2 - k)}, \quad (7)$$



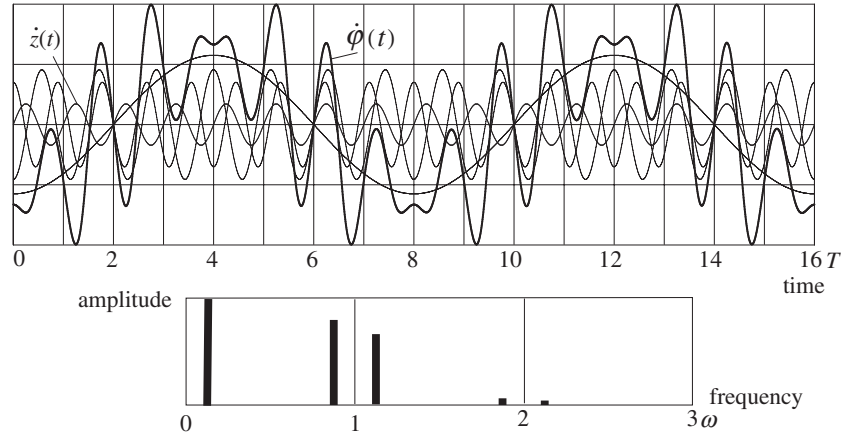


**Figure 3.** Angular velocity  $\dot{\phi}(t)$  time dependence (with the graphs of separate harmonics) and its spectrum for subharmonic resonance of the eighth order.

The fundamental harmonic whose period equals eight driving periods dominates the spectrum. We may treat it as a subharmonic (as an ‘undertone’) of the driving oscillation. This principal harmonic of the frequency  $\omega/n$  describes the smooth component  $\psi(t)$  of the compound period-8 oscillation:  $\psi(t) = A \sin(\omega t/n)$ .

The threshold conditions for stabilization of the inverted pendulum correspond to a slow oscillation of an indefinitely long period about  $\psi = \pi$ . Such an oscillation can be regarded as a subharmonic oscillation of the inverted pendulum whose order  $n$  tends to infinity. Therefore, the desired criterion of stability can be found from the conditions of  $n$ -order subharmonic resonance in the limit  $n \rightarrow \infty$ . Next we try to find these conditions for the subharmonic resonance of arbitrary order  $n$ , valid, in particular, for relatively low frequencies and large amplitudes of the excitation.

When the drive amplitude is slightly greater than the threshold for the subharmonic resonance of order  $n$ , the pendulum angular excursion is small, and we can replace  $\sin \psi$  by  $\psi$  in expression (3) for the momentary angle of deflection  $\varphi(t)$ :

$$\varphi(t) \approx \psi(t) - \frac{a}{l} \sin \psi(t) \cos \omega t \approx \psi(t) - m\psi(t) \cos \omega t, \quad m = \frac{a}{l}. \quad (8)$$

This means that the spectrum of  $n$ -periodic oscillations of a small amplitude consists of the principal harmonic  $A \sin(\omega t/n)$  with the frequency  $\omega/n$  and two higher harmonics of order  $n - 1$  and  $n + 1$  with equal amplitudes:

$$\begin{aligned} \varphi(t) &= A \sin\left(\frac{\omega}{n}t\right) - mA \sin\left(\frac{\omega}{n}t\right) \cos \omega t \\ &= A \sin\left(\frac{\omega}{n}t\right) + \frac{mA}{2} \sin\left(\frac{n-1}{n}\omega t\right) - \frac{mA}{2} \sin\left(\frac{n+1}{n}\omega t\right). \end{aligned} \quad (9)$$

This spectral composition is in general supported by the plots in figure 3 obtained by numerical integration of the exact differential equation (2). It may seem strange that the harmonic component of order  $n$  with the frequency of excitation is absent in the spectrum. However, this peculiarity is easily explained. Indeed, the rapid component  $\cos \omega t$  enters  $\varphi(t)$  being multiplied by  $\sin \psi(t) \approx \psi(t)$ , that is, it has a slow varying amplitude that changes sign each time the pendulum crosses the equilibrium position. This means that the oscillation

with frequency  $\omega$  of the excitation is not a harmonic of  $\varphi(t)$ , because harmonics of a periodic function must have constant amplitudes.

When the pendulum crosses the equilibrium position, the high harmonics of orders  $n - 1$  and  $n + 1$  add in the opposite phases and almost do not distort the graph of the smooth motion (described by the principal harmonic). Near the utmost deflections of the pendulum, the phases of both high harmonics coincide and distort noticeably the slow component.

According to equation (9), both high harmonics have equal amplitudes  $(m/2)A$ . However, we see from the plots in figure 3 that in the actual motion of the pendulum these amplitudes are slightly different. Therefore, we can try to improve the approximate solution for  $\varphi(t)$ , equation (9), as well as the theoretical threshold values of  $m$  for the excitation of subharmonic resonances, by assuming for an improved solution a similar spectrum but with unequal amplitudes,  $A_{n-1}$  and  $A_{n+1}$ , of the two high harmonics (for  $n > 2$ , the case of  $n = 2$  will be considered separately). Moreover, figure 3 shows small contributions in  $\varphi(t)$  of harmonics with frequencies  $(2n - 1)\omega/n$  and  $(2n + 1)\omega/n$ , which we also include in the trial function:

$$\begin{aligned} \varphi(t) = & A_1 \sin(\omega t/n) + A_{n-1} \sin[(n-1)\omega t/n] + A_{n+1} \sin[(n+1)\omega t/n] \\ & + A_{2n-1} \sin[(2n-1)\omega t/n] + A_{2n+1} \sin[(2n+1)\omega t/n]. \end{aligned} \quad (10)$$

Since oscillations at the threshold of excitation have infinitely small amplitudes, we can use instead of equation (2) the following linearized (Mathieu) equation:

$$\ddot{\varphi} + 2\gamma\dot{\varphi} + \omega^2(k - m \cos \omega t)\varphi = 0, \quad (m = a/l). \quad (11)$$

Here we have used the parameter  $k = g/(l\omega^2)$  introduced by (6). The absolute minimum of the driving amplitude  $m$  for excitation of a subharmonic resonance is achieved in the absence of friction at  $\gamma = 0$ . Substituting  $\varphi(t)$ , equation (10), into this equation (with  $\gamma = 0$ ) and expanding the products of trigonometric functions, we obtain the following system of approximate equations for the coefficients  $A_1$ ,  $A_{n-1}$  and  $A_{n+1}$ ,  $A_{2n-1}$  and  $A_{2n+1}$ :

$$\begin{aligned} 2(kn^2 - 1)A_1 + mn^2A_{n-1} - mn^2A_{n+1} &= 0, \\ mn^2A_1 + 2[n^2(k-1) + 2n-1]A_{n-1} - mn^2A_{2n-1} &= 0, \\ -mn^2A_1 + 2[n^2(k-1) - 2n-1]A_{n+1} + mn^2A_{2n+1} &= 0, \\ mn^2A_{n-1} + 2[n^2(k-4) + 4n-1]A_{2n-1} &= 0, \\ mn^2A_{n+1} + 2[n^2(k-4) - 4n-1]A_{2n+1} &= 0. \end{aligned} \quad (12)$$

The homogeneous system (12) has a nontrivial solution if its determinant equals zero. This condition yields an equation (not cited here) for the corresponding threshold (minimal) normalized driving amplitude  $m_{\min} = a_{\min}/l$  at which  $n$ -periodic mode  $\varphi(t)$  given by expression (10) can exist. (This equation can be solved with the help of, say, *Mathematica* package by Wolfram Research, Inc.) Then, after substituting this critical driving amplitude  $m_{\min}$  into (12), fractional amplitudes  $A_{n-1}/A_1$ ,  $A_{n+1}/A_1$ ,  $A_{2n-1}/A_1$  and  $A_{2n+1}/A_1$  of high harmonics for a given order  $n$  can be found as the solutions to the homogeneous system of equations (12).

If we ignore the contribution of harmonics with frequencies  $(2n - 1)\omega/n$  and  $(2n + 1)\omega/n$  in  $\varphi(t)$ , that is, assume  $A_{2n-1}$  and  $A_{2n+1}$  to be zero, system (12) simplifies considerably. The corresponding approximate solution can be found in [9]. For the full system (12), the final expressions for  $m_{\min}$  and for the amplitudes of harmonics are too bulky to be cited here. We have used them in figure 4 for plotting the curves of  $m_{\min}$  as functions of  $k = (\omega_0/\omega)^2$  (inverse normalized driving frequency squared) corresponding to subharmonic oscillations of different orders  $n$  (thin curves).

To verify our analytical results for subharmonic oscillations in a computer simulation, we choose a value  $k = -0.3$ , corresponding to the drive frequency  $\omega = 1.826\omega_0$  for which

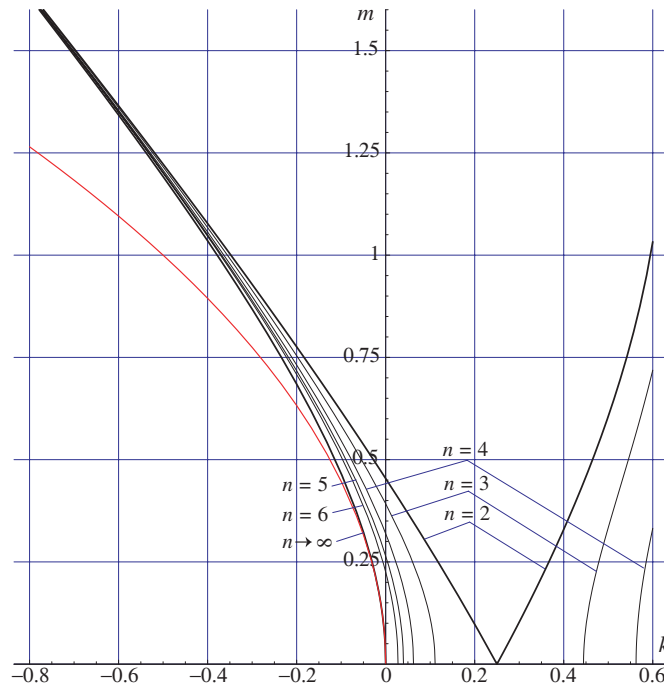


**Figure 4.** The normalized driving amplitude  $m = a/l$  versus  $k = (\omega_0/\omega)^2$  (inverse normalized driving frequency squared) at the lower boundary of the dynamic stabilization of the inverted pendulum (the left curve marked as  $n \rightarrow \infty$ ), and at subharmonic resonances of several orders  $n$  (see the text for details).

(This figure is in colour only in the electronic version)

the separation of slow and rapid motions of the pendulum is obviously inapplicable. The above-described calculation for the subharmonic oscillation of order  $n = 8$  predicts for the threshold normalized drive amplitude  $m_{\min} = a_{\min}/l$  a value 87.73% of the pendulum length. The simulation presented in figure 5 perfectly confirms this theoretical prediction. The set of Poincaré sections in the phase plane consists of eight fixed points, and the phase orbit becomes closed after eight cycles of the pivot oscillations. The fractional amplitudes of harmonics obtained in the simulation agree perfectly well with the theoretical prediction.

### 6. The lower boundary of dynamic stabilization

As we already noted, the criterion of stability for the inverted pendulum can be related to the condition of subharmonic resonances of an infinitely large order  $n$  in the vicinity of  $\varphi = \pm\pi$ . Hence, the limit of  $m_{\min}$  at  $n \rightarrow \infty$  gives an improved formula for the lower boundary of dynamic stabilization of the inverted pendulum. If we use the approximate solution of (12) in which the contribution of higher harmonics with frequencies  $(2n - 1)\omega/n$  and  $(2n + 1)\omega/n$  is ignored, the limit  $n \rightarrow \infty$  gives for the lower boundary the value  $m_{\min} = \sqrt{-2k(1 - k)}$  in the region  $k < 0$  (see [9]). For the solution of the full system (12) with higher harmonics included, the limit of  $m_{\min}$  at  $n \rightarrow \infty$  yields the following expression:

$$m_{\min} = 2\sqrt{\frac{k(k - 1)(k - 4)}{3k - 8}}, \tag{13}$$

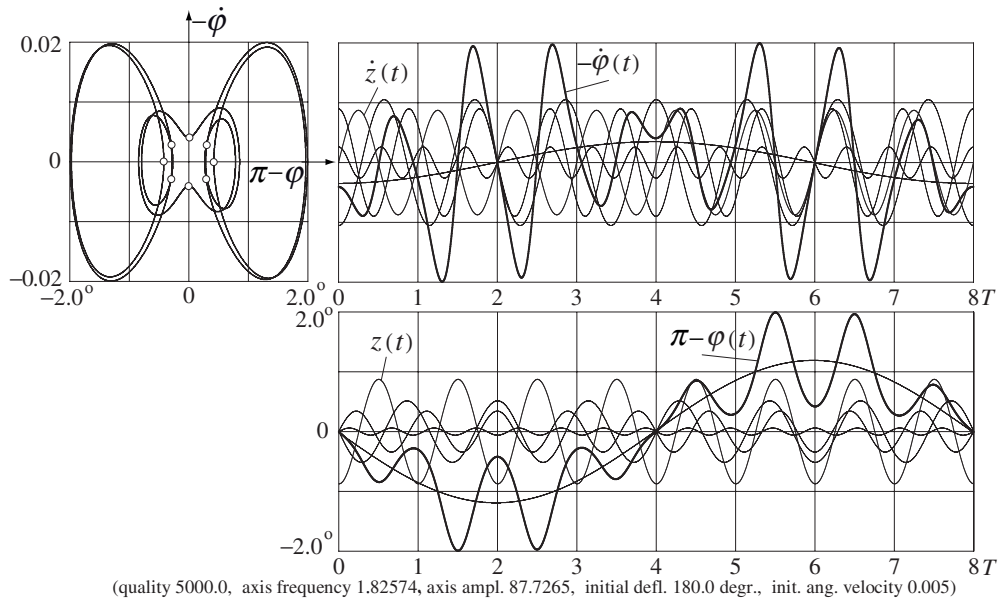


**Figure 5.** Phase trajectory with Poincaré sections, angular velocity  $-\dot{\varphi}(t)$  and angle  $\pi - \varphi(t)$  time dependences (with the graphs of separate harmonics) for subharmonic resonance of the eighth order. For convenience of presentation, the angle is measured from the inverted position.

which should be used instead of the commonly known approximate criterion  $m_{\min} = \sqrt{-2k}$  given by equation (5). The minimal amplitude  $m_{\min} = a_{\min}/l$  that corresponds to the improved criterion (13) of dynamic stabilization is shown as a function of  $k = (\omega_0/\omega)^2$  by the thick left curve marked as  $n \rightarrow \infty$  in figure 4. This curve is localized wholly in the region of negative  $k$  values. To compare the improved criterion (13) with the commonly known criterion (5) of the inverted pendulum stability, the latter is also shown in figure 4 by the thin curve (red in the electronic version). We note how these two curves diverge dramatically at low frequencies and large amplitudes of the pivot oscillations.

The other curves to the right from this boundary show the dependence on  $k$  of minimal driving amplitudes for which the subharmonic resonances of several orders can exist (the first curve for  $n = 6$ , and the others for  $n$  values diminishing down to  $n = 2$  from left to right). At negative  $k$  values, these curves give the threshold drive amplitudes for subharmonic oscillations about the inverted position. Case  $k = 0$  corresponds to zero gravity (or infinitely high drive frequency). Points of intersection of the curves with the ordinate axis on this diagram give minimal drive amplitudes for which in the absence of gravity subharmonic oscillations of certain order,  $n$  can exist about any of the two dynamically stabilized positions (figure 2 shows an example of such period-8 oscillations).

Continuations of the curves to positive  $k$  values correspond to subharmonic parametric resonances ('multiple-nodding' oscillations) about the downward equilibrium position. The curve for  $n = 2$  corresponds to ordinary parametric resonance in which two cycles of excitation take place during one full oscillation of the pendulum. In the absence of friction, the threshold drive amplitude for this resonance tends to zero at  $\omega \rightarrow \omega_0/2$ , that is, at  $k \rightarrow 1/4$ . From figure 4 we see clearly that the curve, corresponding to  $n = 2$  subharmonic oscillations of the inverted pendulum ('flutter' mode), and the principal parametric resonance of ordinary

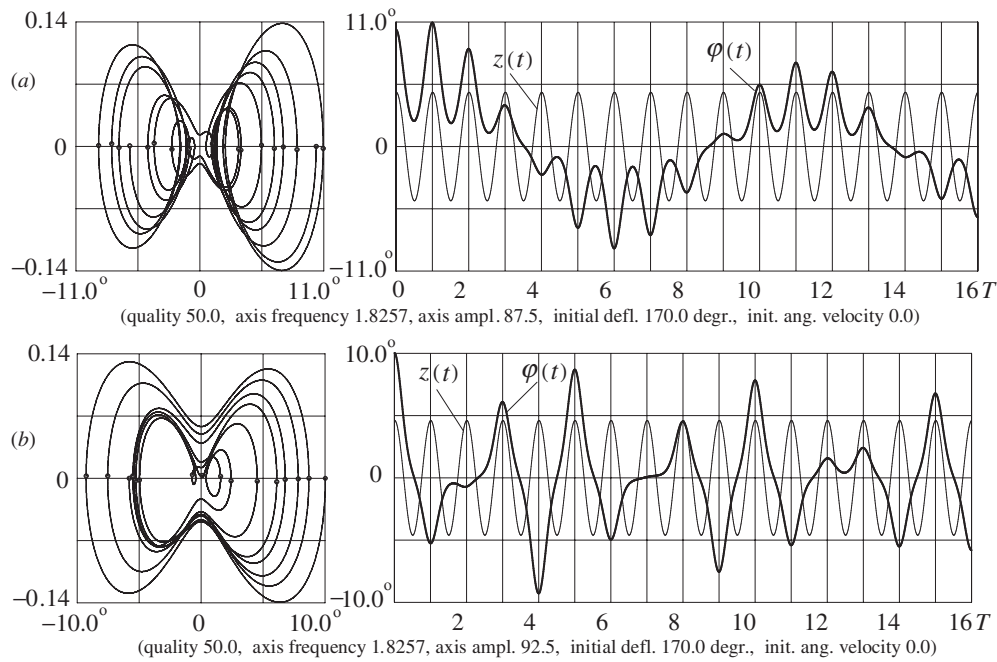


**Figure 6.** Phase trajectories and time histories of gradually damping oscillations about the inverted position just over the lower (a) and just below the upper (b) boundaries of dynamic stabilization.

(hanging) pendulum belong to the essentially same branch of period-2 regular behavior. In the  $k < 0$  region, this branch gives the upper boundary of dynamic stabilization for the inverted pendulum (see section 7).

We note that the existence of subharmonic oscillations in the same region of the  $k$ - $m$  plane does not disprove criterion (13) of the inverted pendulum stability. Indeed, the pendulum is trapped into the  $n$ -periodic subharmonic limit cycle (with  $n > 2$ ) only if the initial state belongs to a certain small basin of attraction that corresponds to this limit cycle. Otherwise the pendulum eventually comes to rest in the inverted position (or to unidirectional rotation, if the pendulum is released beyond certain critical initial deviation).

For experimental verification of the improved criterion (13) we choose again relatively low drive frequency  $\omega = 1.826 \omega_0$  ( $k = -0.3$ ) for which distinctions between the conventional and improved criteria are especially noticeable. At this frequency (13) gives for the lower boundary of stability, the drive amplitude  $a_{\min} = 0.868l$ . The upper boundary (see section 7) at  $k = -0.3$  equals  $a_{\max} = 0.929l$ . Computer simulations in figure 6 show how within this narrow region of stability at  $a = 0.875l$  (just over the lower boundary, figure 6(a)) and at  $a = 0.925l$  (just below the upper boundary, figure 6(b)), the pendulum, being initially deviated through  $10^\circ$  and released with zero velocity, returns gradually to the inverted position. If the initial deflection exceeds some critical value, at first the pendulum goes slowly further from the vertical, then executes random revolutions to one and the other side, and eventually (after a long ‘tumbling’ chaotic transient) becomes trapped into period-1 unidirectional rotation. The closer the drive parameters to the boundary of stability, the smaller this critical deviation. For  $k = -0.3$ ,  $m = 0.875$  and  $Q = 50$  the initial deviation from the inverted position should not exceed  $14^\circ$ . Friction reduces the basin of attraction of the equilibrium in the inverted state: at  $Q = 20$  the initial deviation should not exceed  $10^\circ$ .

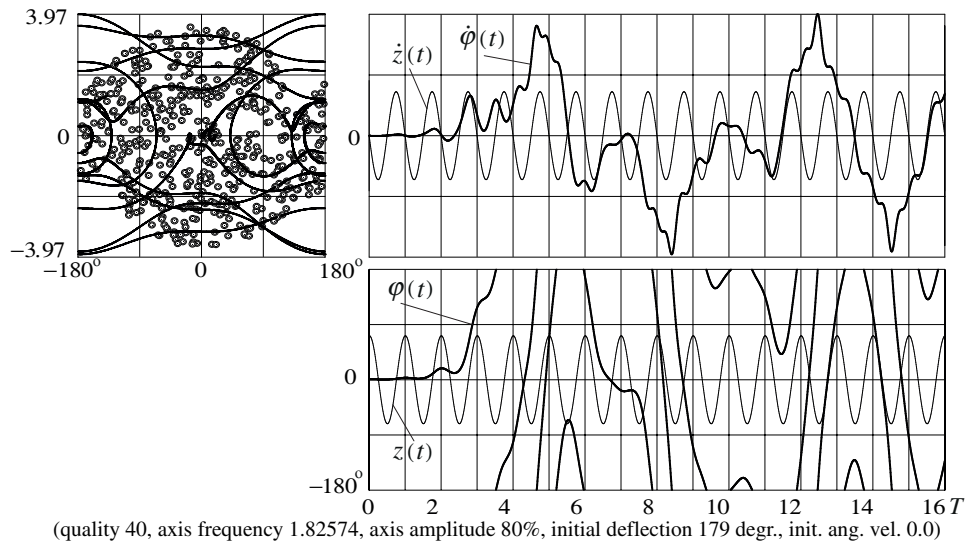


Figure 7. Chaotic oscillations below the boundary of stability.

We note the peculiarities of the transients shown in figure 6 that lead to the state of rest in the inverted position. In both cases, Poincaré sections, corresponding to time instants  $t_q = qT$  ( $q = 0, 1, 2 \dots, T = 2\pi/\omega$ —period of the pivot oscillations), are located near the  $\varphi$ -axis and gradually condense, approaching the origin of the phase plane. Near the lower boundary of stability, the graph of time history in figure 6(a) resembles, during a limited time interval, the corresponding graph of a subharmonic resonance (‘multiple-nodding’ oscillation) of some high order (compare with figure 5): the pendulum executes many ‘nods’ on one side of the inverted position, then on the other side with a somewhat smaller amplitude, and so on, approaching gradually the vertical. These intermittent damping ‘nods’ are described by one-sided shrinking loops of the phase orbit that pass from one side of the phase plane to the other each time the pendulum crosses the vertical line. Near the upper boundary, the graph of time history and the phase trajectory (figure 6(b)) resemble those of a ‘flutter’ oscillation (see section 7): one cycle of the pendulum covers approximately two drive periods and is represented by a double-lobed phase orbit (compare with figure 10). This orbit shrinks gradually around the origin of the phase plane.

At smaller than  $0.868l$  values of the drive amplitude the inverted pendulum is unstable. Figure 7 shows how at  $k = -0.3$  and  $a = 0.800l$  the pendulum, being released at only  $1^\circ$  deviation from the inverted position, occurs eventually in a chaotic regime (‘tumbling’ chaos). The graphs in figure 7 show the initial stage of the time history. The set of Poincaré sections in the phase plane gives impression of the further random behavior, characterized by a strange attractor. We note that the inverted pendulum at these drive parameters should be stable according to conventional criterion (5), which at  $k = -0.3$  gives a considerably smaller value  $a_{\min} = 0.775l$  (compare with the improved value  $a_{\min} = 0.868l$ ) for the lower boundary of stability.

### 7. The upper boundary of dynamic stabilization

The curve  $n = 2$  in figure 4 (its part in the  $k \leq 0$  region) corresponds to the upper boundary of dynamic stabilization for the inverted pendulum: after a disturbance the pendulum does not

come to rest in the up position, no matter how small the release angle, but instead eventually settles into a limit cycle, executing finite amplitude steady-state oscillation (about the inverted vertical position). The period of such an oscillation is twice the driving period, and its swing grows as the excess of the drive amplitude over the threshold  $a_{\max}$  is increased.

This loss of stability of the inverted pendulum was first described in 1992 by Blackburn *et al* [5] and demonstrated experimentally in [6]. The authors [5] called these limit-cycle oscillations the ‘flutter’ mode. Because the ‘flutter’ mode and the principal parametric resonance belong to the same branch of period-2 stationary regime (this unambiguously follows from figure 4), the same analytical method can be used to calculate conditions of their excitation. Simulations show a very simple spectral composition for both, namely a superposition of the fundamental harmonic whose frequency  $\omega/2$  equals half the driving frequency, the third harmonic with the frequency  $3\omega/2$ , and maybe a tiny admixture of the fifth harmonic:

$$\varphi(t) = A_1 \cos(\omega t/2) + A_3 \cos(3\omega t/2) + A_5 \cos(5\omega t/2). \quad (14)$$

The phases of harmonics in (14) correspond to pivot oscillations in the form  $z(t) = a \cos \omega t$ . Substituting  $\varphi(t)$  into the differential equation (11) with  $\gamma = 0$  and expanding the products of trigonometric functions, we obtain an expression in which we should equate to zero the coefficients of  $\cos(\omega t/2)$ ,  $\cos(3\omega t/2)$ , and  $\cos(5\omega t/2)$ . Thus, we get a system of homogeneous equations for the coefficients  $A_1$ ,  $A_3$  and  $A_5$  of harmonics in the trial function (14):

$$\begin{aligned} (4k - 2m - 1)A_1 - 2mA_3 &= 0, \\ -2A_1 + (4k - 9)A_3 - 2mA_5 &= 0, \\ -2mA_3 + (4k - 25)A_5 &= 0. \end{aligned} \quad (15)$$

This system has a nontrivial solution when its determinant equals zero. If we neglect the contribution of the fifth harmonic in  $\varphi(t)$ , equation (14), that is, let  $A_5 = 0$ , we get the following approximate expression for the upper boundary of stability:

$$m_{\max} = \frac{1}{4}[\sqrt{(4k - 9)(20k - 13)} + 4k - 9]. \quad (16)$$

If the fifth harmonic is included, the requirement for the nontrivial solution to the system (15) yields a cubic equation for the desired normalized critical driving amplitude  $a_{\max}/l = m_{\max}$ . The relevant root of this equation (too cumbersome to be shown here) is used for plotting the curve  $n = 2$  in figure 4. However, for the interval of  $k$  values under consideration ( $-0.8$ – $0.6$ ), the approximate expression (16) gives a curve which is visually indistinguishable from the curve  $n = 2$  in figure 4.

The curve  $n = 2$  intersects the ordinate axis at  $m \approx 3(\sqrt{13} - 3)/4 = 0.454$ . This case ( $k = 0$ ) corresponds to the above-mentioned limit of a very high driving frequency ( $\omega/\omega_0 \rightarrow \infty$ ) or zero gravity ( $\omega_0 = 0$ ), so that  $m = 0.454$  gives the upper limit of stability for each of the two dynamically stabilized equivalent equilibrium positions: if  $m > 0.454$  at  $g = 0$ , the flutter mode is excited.

The lower and upper boundaries of the dynamical stability gradually converge while the drive frequency is reduced: figure 4 shows that the interval between  $m_{\min}$  and  $m_{\max}$  shrinks to the left, when  $|k|$  is increased. Both boundaries merge at  $k \approx -1.41$  ( $\omega \approx 0.8423\omega_0$ ) and  $m \approx 2.451$ . The diminishing island of the inverted state stability vanishes in the surrounding sea of chaotic motions.

The improved theoretical values for the lower and upper boundaries of stability are obtained here for the frictionless system ( $\gamma = 0$ ). Computer simulations (based on numerical integration of the exact differential equation (2)) show that relatively weak friction

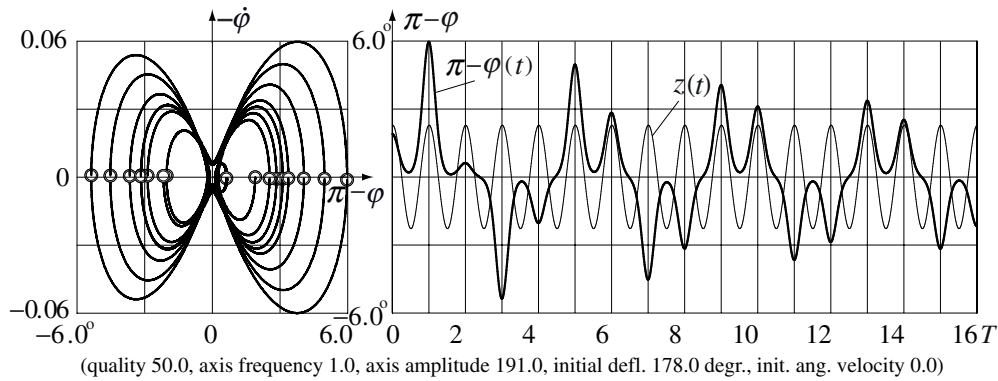


Figure 8. Dynamical stability at low frequency and large amplitude of the drive.

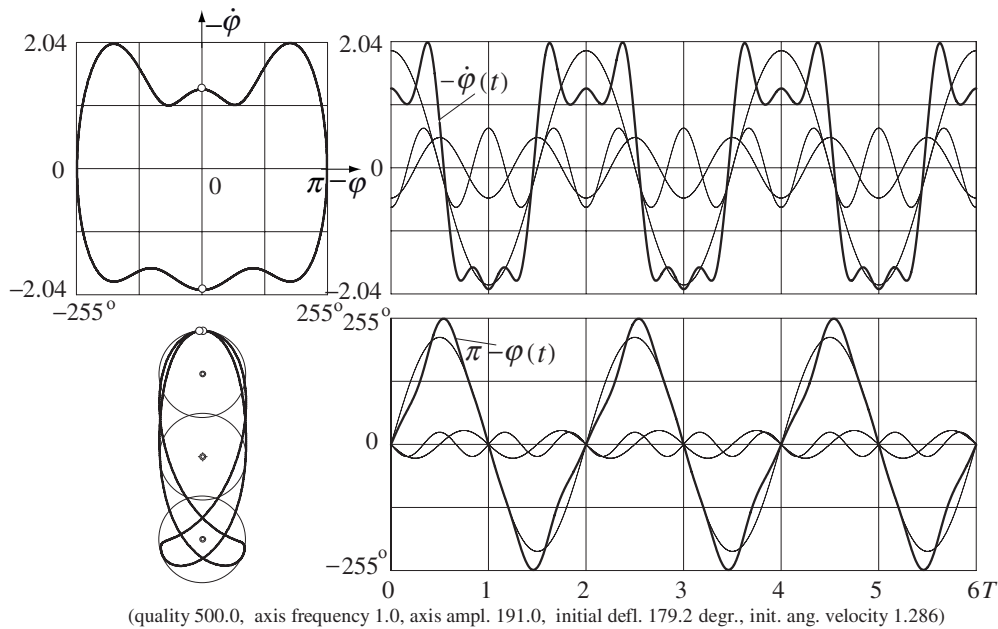
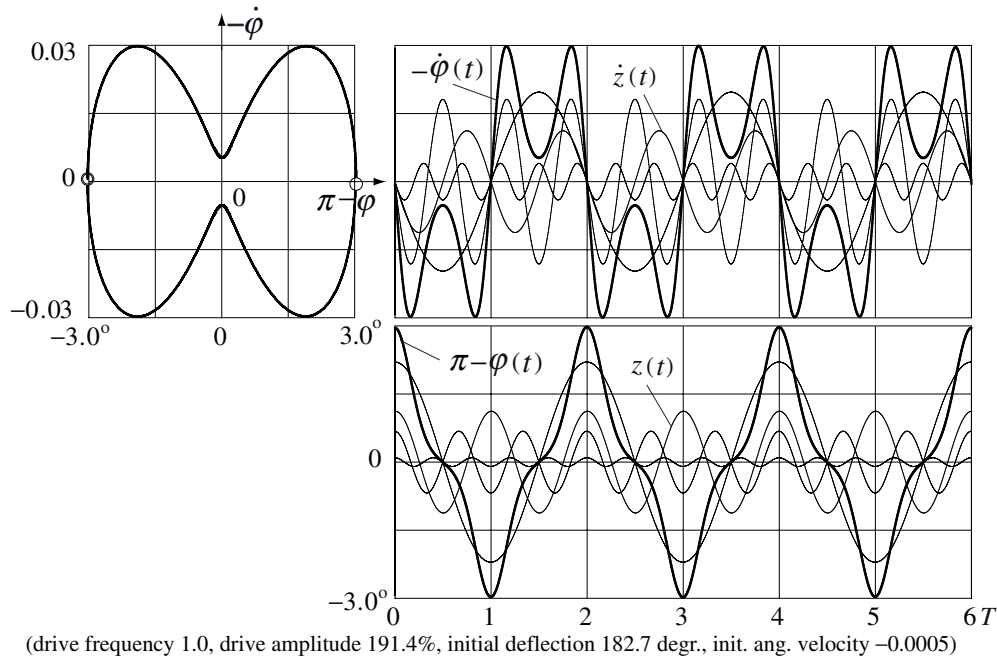


Figure 9. Period-2 oscillation of a large amplitude about the inverted position: the phase orbit, spatial trajectory, and graphs of angular velocity  $\dot{\varphi}(t)$  and angle  $\varphi(t)$  time dependences (with the graphs of separate harmonics).

( $Q \geq 15-30$ ) does not influence noticeably these boundaries. This can be easily explained physically if we take into account that in conditions of dynamical stabilization (sufficiently large frequency or amplitude of excitation), the role of inertial forces is much more important. In contrast, the basin of attraction for the pendulum equilibrium in the inverted position is sensitive to friction: the interval of initial deviations within which the pendulum returns eventually to the inverted position becomes smaller as friction is increased.

For further experimental verification of the improved values for both upper and lower boundaries of the inverted pendulum stability, and for comparison of the criterion (13) with the conventional one (5), we now choose  $k = -0.5$  (drive frequency  $\omega = 1.4142\omega_0$ ).



**Figure 10.** The phase orbit and graphs of  $\varphi(t)$  and  $\dot{\varphi}(t)$  for ‘flutter’ oscillations of the inverted pendulum just over the upper boundary of stability.

For this  $k$  value criterion, (13) yields  $m_{\min} = 1.1920$  (119.20% of the pendulum length), while (5) gives  $m_{\min} = 1.00$  ( $a_{\min} = l$ ) – 100%. The theoretical value for the upper boundary at  $k = -0.5$  is  $m_{\max} = 1.2226$  (122.26%), while according to (16)  $m_{\max} = 1.2265$  (122.65%). Simulations show that below  $m = 115.68\%$ , the motion is chaotic (‘tumbling’ chaos), at  $m = 115.69$ – $119.19\%$  the pendulum, after a long chaotic transient, is trapped in period-1 non-uniform unidirectional rotation (in contradiction with conventional criterion (5), which predicts stability of the inverted position), and only in the interval  $m = 119.20$ – $122.27\%$  the pendulum, being released at a small deviation from the inverted position, eventually comes to rest, in exact accordance with the improved criterion (13). Then, over the upper boundary of stability, at  $m = 122.28$ – $123.02\%$  the pendulum occurs in a ‘flutter’ mode; at  $m = 123.03$ – $147.01\%$  executes unidirectional rotation; at  $m = 147.02$ – $150.6\%$  the pendulum, after a long chaotic transient, comes to period-2 oscillation about the inverted position with an amplitude of approximately  $260^\circ$  (similar to the oscillation shown in figure 9); at  $m \geq 150.7\%$  the pendulum eventually settles into the unidirectional rotation.

Further simulations refer to the case of especially low frequency of the pivot oscillations:  $\omega = \omega_0$  ( $k = -1$ ). The theoretical values for the lower and upper boundaries of stability for this frequency are  $m_{\min} = 1.9069$  (190.69% of the pendulum length) and  $m_{\max} = 1.9138$  (191.38%), respectively. Figure 8 shows how in this narrow interval the pendulum, being released at  $178^\circ$ , first goes further from the vertical for about  $6^\circ$  maximum angular excursion and then gradually approaches the inverted position by the process of irregular damping oscillations. The basin of attraction for equilibrium in the inverted position is rather small: at slightly different initial conditions, the pendulum, after a long transient, occurs in a steady-state large-amplitude (approximately  $255^\circ$ ) period-2 oscillation about the inverted position.

The angular excursion of the pendulum from one extreme position to the other takes one period of excitation and is greater than a full circle (about  $510^\circ$ ). Therefore, otherwise we can treat this regime as alternating clockwise and counterclockwise revolutions. The phase orbit (with two fixed points of Poincaré sections) and the spatial trajectory of the pendulum bob in figure 9 give an impression of such an extraordinary pendulum motion, which coexists with the state of rest in the inverted position. Just over the upper boundary of stability (191.38%), the pendulum eventually settles into the ‘flutter’ mode (figure 10).

## 8. Concluding remarks

The commonly known criterion for dynamic stabilization of the inverted pendulum is usually derived by separation of rapid and slow motions of the pendulum. This approach and related concept of the effective potential for the slow motion are very useful for physical explanation of the dynamic stabilization, as well as of the origin of subharmonic resonances of high orders. However, this separation of rapid and slow motions is admissible only at sufficiently high frequency and small amplitude of the pivot oscillations.

An improved criterion for the lower boundary of dynamic stabilization, valid in a wider region of frequencies and amplitudes of the pivot oscillations, including values for which the method of separation of rapid and slow motions is inapplicable, is obtained by establishing a close relationship between the phenomenon of dynamic stabilization of the inverted pendulum and subharmonic resonances.

The upper boundary of stabilization is related to the excitation of period-2 ‘flutter’ oscillation, which is a complete analog of the principal parametric resonance. Both phenomena belong to the same branch of stationary period-2 oscillations, and the criterion for destabilization of the inverted position is obtained by the same method as for the excitation of ordinary parametric resonance. Results of corresponding analytical calculations agree perfectly well with computer simulations.

## References

- [1] Stephenson A 1908 On an induced stability *Phil. Mag.* **15** 233–6
- [2] Kapitza P L 1951 Dynamic stability of the pendulum with vibrating suspension point *Sov. Phys.—JETP* **21** 588–97 (in Russian)  
Kapitza P L 1965 *Collected Papers of P. L. Kapitza* vol 2, ed D Ter Haar (London: Pergamon) pp 714–26
- [3] Landau L D and Lifschitz E M 1988 *Mechanics* (Moscow: Nauka) pp 123–5 (in Russian)  
Landau L D and Lifschitz E M 1976 *Mechanics* (New York: Pergamon) pp 93–5
- [4] Broer H W, Hoveijn I, van Noort M, Simó C and Vegter G 2004 The parametrically forced pendulum: a case study in  $1\frac{1}{2}$  degree of freedom *J. Dyn. Differ. Eqns* **16** 897–947
- [5] Blackburn J A, Smith H J T and Groenbech-Jensen N 1992 Stability and Hopf bifurcations in an inverted pendulum *Am. J. Phys.* **60** 903–8
- [6] Smith H J T and Blackburn J A 1992 Experimental study of an inverted pendulum *Am. J. Phys.* **60** 909–11
- [7] Acheson D J 1995 Multiple-nodding oscillations of a driven inverted pendulum *Proc. R. Soc. A* **448** 89–95
- [8] Butikov E I 2001 On the dynamic stabilization of an inverted pendulum *Am. J. Phys.* **69** 755–68
- [9] Butikov E I 2002 Subharmonic resonances of the parametrically driven pendulum *J. Phys. A: Math. Gen.* **35** 6209–31